

# Non-Linear Local Force Feedback Control for Haptic Interfaces <sup>★</sup>

Ribin Balachandran <sup>\*</sup> Natalia Kozlova <sup>\*</sup> Christian Ott <sup>\*</sup>  
Alin Albu-Schaeffer <sup>\*,\*\*</sup>

<sup>\*</sup> German Aerospace Center (DLR), Wessling, Germany (e-mail:  
Ribin.Balachandran@dlr.de, Natalia.Kozlova@dlr.de,  
Christian.Ott@dlr.de)

<sup>\*\*</sup> Technical University of Munich, Germany (e-mail:  
Alin.Albu-Schaeffer@dlr.de)

---

**Abstract:** In this paper, a time-continuous, non-linear local force feedback control is proposed which produces low inertia of the haptic interface during free slave motion as well as higher transparency during slave-environment interactions, by modifying the local force gain as a function of the measured forces of the slave-environment interaction. Stability of the system is proven using damping injection based on a model-based passivation approach and a model-free time domain passivity approach. Teleoperation experiments with time-delay on a KUKA light weight robot-based master device show improvements in performance while using the proposed method.

*Keywords:* Non-linear force control, feedforward control, teleoperation, haptics, time delay

---

## 1. INTRODUCTION

Telepresence enables the control of a remote robot by a human operator using a haptic interface. The feedback of forces from the remote robot (*slave*) interacting with its environment improves the dexterity levels and telemanipulation performance of the operator. The haptic device (*master*) with the bilateral controller should ideally reproduce *only* the slave-environment interactions to the operator through which he feels he is directly interacting with the environment. Ranging from extremely light devices like sigma.7 described in Tobergte et al. (2011) to more massive systems like in the DLR teleoperation facility HUG as in Hulin et al. (2011), several designs for haptic interfaces and bilateral controllers have been studied and reported in Hokayem and Spong (2006). DLR-HUG is a bi-manual robotic facility to test haptic and teleoperation algorithms which has master devices comprised of KUKA Light Weight Robots (LWR) transformed as haptic devices and is shown in Fig. 1. The benefits of such massive systems are larger work-spaces and higher levels of force interaction.

On the other hand, due to the massive structure and high physical damping, these devices demand higher physical effort from the operator, especially while telemanipulating similarly massive slave devices. Fig. 1 shows a human operator telemanipulating the DLR-HUG bi-manual haptic device along with the slave robot which has LWR based arms. Force-torque sensors attached to the haptic interface's end-effector enable local force feedback control which reduces the apparent inertia of the system perceived by the operator.

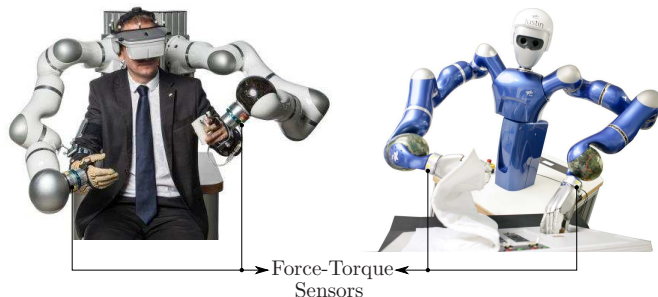


Fig. 1. KUKA light weight robots used as haptic interfaces in DLR-HUG (left) and the slave humanoid robot Space-Justin which has LWR based arms (right).

Local force feedback control has been widely used in bilateral controllers to improve the transparency of the haptic system as explained in (Hastrudi-Zaad and Salcudean (1999), Hashtrudi-Zaad and Salcudean (2002) and Ishii and Katsura (2012)) and it has been analytically and experimentally shown in these works that ideal transparency can be achieved only under negligible time-delays. Constant force feedforward gain has been used in Kaneko et al. (1998) to improve the manipulation dexterity while working in different scale worlds. The method in Colgate (1993) alters the impedance of the task and also changes the device dynamics as in Abdossalami and Siropour (2008). A local force feedback scheme has been used in Ueberle and Buss (2002) to compensate gravitational forces. It has also been successfully applied to decrease the perceived inertia of the device in Tobergte et al. (2011) and Gil et al. (2009). In Gil et al. (2009), it is shown that using local force feedback and increasing the stiffness of virtual objects do not affect the stability of the system for only relatively low local force feedback gains.

---

<sup>★</sup> Partially funded by the EU-Horizon 2020 research and innovation program under grant agreement No 644271, AEROARMS project.

All the aforementioned works apply constant gains for local force feedback. The goal of this paper is two-fold<sup>1</sup>: First, a time-continuous, time-varying gain for the local force feedback is proposed which shows better performance compared to conventional methods that use only constant gains. The gain is modified based on the measured forces from the slave-environment interaction which is a simple and heuristic approach to improve the transparency of the system. Second, the stability of the system is ensured using a model-based damping calculation with an energy function and then, Time Domain Passivity Approach (TDPA), a widely used passivity tool, is applied to passivate and stabilize the system.

Sec. 2 introduces the concept of local force feedback control and the major limitation that the authors observe with this approach. In Sec. 3, the new approach with a time-varying non-linear local force feedback gain is described. Sec. 4 covers a discussion about the stability of the proposed method using 2 different approaches. Results of the hardware experiments are given in Sec. 5. Sec. 6 summarizes the work with a brief outlook.

## 2. LOCAL FORCE FEEDBACK CONTROL

### 2.1 Inertia reduction using Constant Local Force Feedback

The signal-flow diagram of a general 4-channel teleoperation system Hastrudi-Zaad and Salcudean (1999) is shown in Fig. 2. The master device is an impedance (mass and physical damping) and the human interacts with it with a force  $F_h$ . The feedback to the master device from the master-side controller is represented by the force  $\tilde{F}_m$ . The slave device interacts with its environment and the measured force  $F_e$  is sent back to the master. The velocities of the master  $V_m$  and the slave  $V_s$  are communicated between the controllers on the corresponding sides.  $T_f$  and  $T_b$  are the communication delays in each direction. The measured

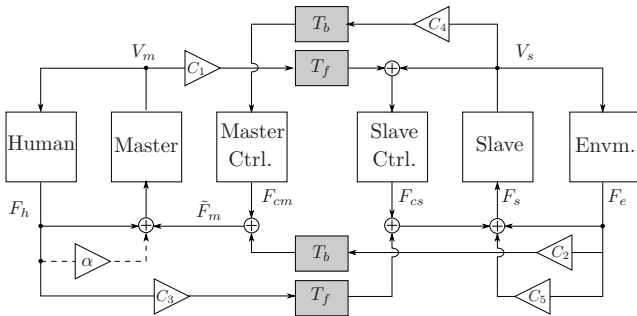


Fig. 2. Signal-flow diagram of 4-channel bilateral controller.

force of the human-master interaction,  $F_h$ , is amplified with a gain  $\alpha$  and is applied to the master device. The amplified human force on the master side then becomes:

$$\tilde{F}_h = F_h + \alpha F_h. \quad (1)$$

One of the conditions for perfect transparency for a non-delayed teleoperation system with 4-channel architecture with local force feedback for the master and the slave

<sup>1</sup> The goal of the paper is not to prove stability for the teleoperation system. It focuses only on the local force feedback concepts which improves the performance of an already stable bilateral controller.

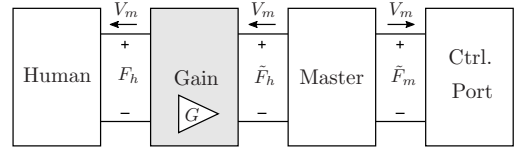


Fig. 3. The reduced model of the teleoperation system with a local force feedback gain.

devices, as mentioned in Hastrudi-Zaad and Salcudean (1999), states that the force feedback gains should satisfy:

$$C_2 = 1 + \alpha, \quad (2)$$

where  $C_2$  is the feedback gain of the measured forces from the slave side. The network representation of the reduced model of the master device interacting with the human and the master controller is shown in Fig. 3. The port named *Gain* introduces a gain  $G = 1 + \alpha$ . The human with the local force feedback gain interacts with the master device through the power-port  $\langle \tilde{F}_h, V_m \rangle$  and the controller port interacts with the master device with  $\langle \tilde{F}_m, V_m \rangle$ .

### 2.2 Motivation and Problem Statement

Experiments with a 4-channel bilateral controller for the LWR-based master device were conducted with local force feedback, with gains satisfying the condition in (2) with and without time-delay. The master device is moved by a human operator trying to follow a desired trajectory (blue dashed line). The position and force signals of the master are commanded to a virtual mass of 2 Kg which collides with a virtual wall of stiffness 1200 N/m. The slave controller forces and the environmental forces are sent back to the master side Artigas et al. (2016). The local force feedback gain for the master device is  $\alpha = 1.4$  and the environmental force feedback gain is 2.4 ( $C_2$ , which satisfies (2)). The corresponding positions  $X_d$ ,  $X_m$ ,  $X_s$  being the desired position trajectory given to the operator, position of the master device, and virtual slave device respectively and measured forces of the master and slave are shown in Fig. 4. It can be seen that the forces of the slave while in contact with the virtual wall (the black line denoted by  $X_w$ ) are perceived by the human with high transparency.

When it comes to teleoperation with communication delay, it will be difficult to satisfy the condition in (2). As it is pointed out in Hastrudi-Zaad and Salcudean (1999), perfect transparency cannot be achieved and the system gets unstable with high values of the measured slave force feedback gain  $C_2$ . Although the effects of time-delay can be removed using passivity based tools like wave-variables Niemeyer and Slotine (1991) or TDPA Artigas et al. (2016), the gain margins are limited as explained in Panzirsch et al. (2016). It can be seen in Fig. 5 that the contact with the virtual wall makes the system highly unstable with a round-trip delay of 30 ms for the same measured force feedback gain  $C_2 = 2.4$ .

So, for teleoperation systems with time delay, the feedback gain of the environmental forces has to be reduced considerably (for example,  $C_2 = 1.0$ ), while  $\alpha$  is still 1.4, thus violating (2). In the next experiment, the controller gains are tuned to make a stable teleoperation system

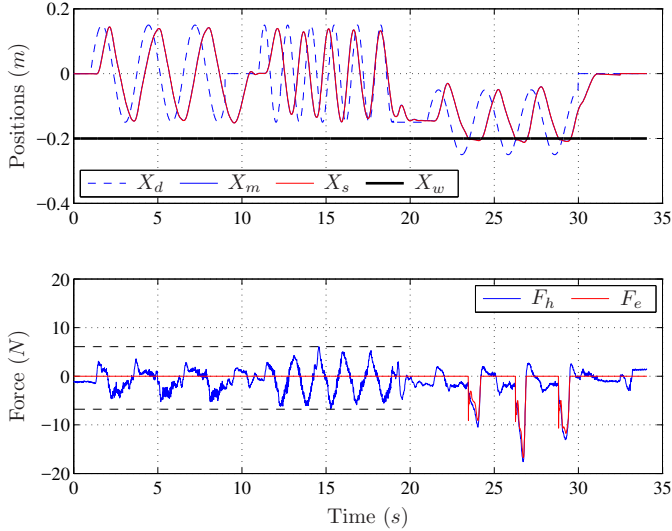


Fig. 4. Positions and forces of the devices with local force feedback control, without delay,  $\alpha=1.4$  and  $C_2=2.4$ . Note that positions  $X_m$  and  $X_s$  are almost identical that it is hard to differentiate them.

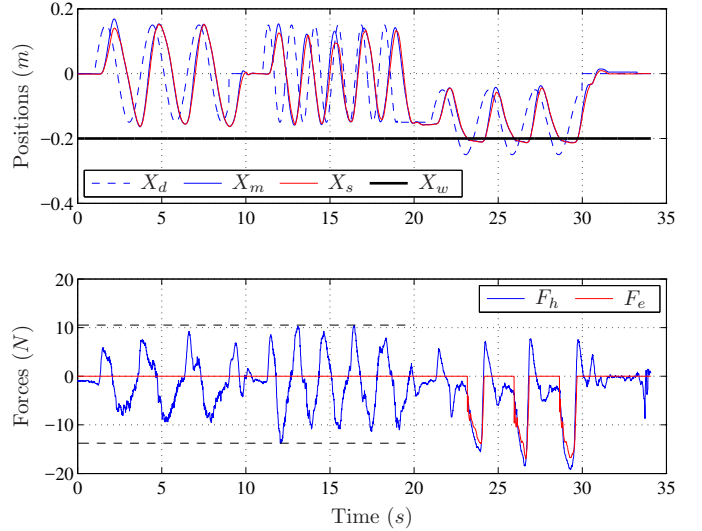


Fig. 6. Positions and forces of the devices without local force feedback, a round-trip delay of 30 ms,  $C_2 = 1.0$ . Note the high  $F_h$  values in free motion, but better force tracking during contacts.

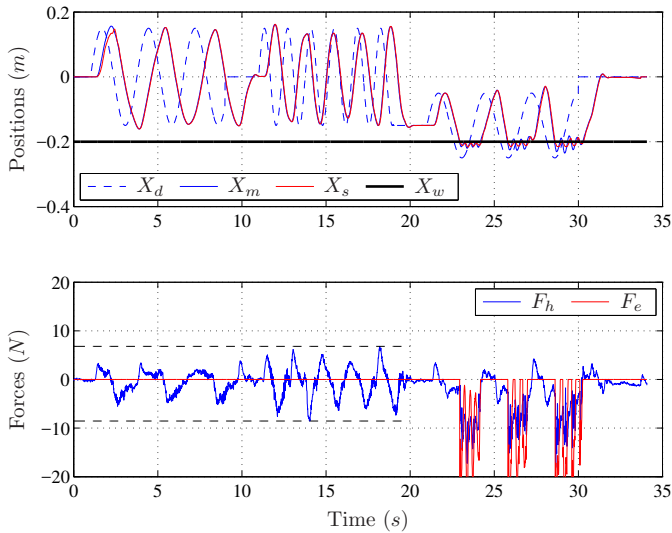


Fig. 5. Positions and forces of the devices with local force feedback and with a round-trip delay of 30 ms,  $\alpha=1.4$  and  $C_2=2.4$ . It can be seen that the contacts get highly unstable.

where the destabilizing effects of time delay are removed using TDPA as explained in Artigas et al. (2016). Fig. 6 shows the system with 30 ms round-trip delay and without local force feedback. It can be seen that although the human operator needs to apply high forces in the free slave motion, the contacts are perceived well at the master side. Now compare this with Fig. 7 which shows the results of the same system applying a local force feedback with constant gain. It can be seen that the human needs to apply lower forces during free motion. But the force measured by the human is reduced significantly when the slave contacts the virtual wall, which is observed by the low force values at the human side (blue) as compared to the slave forces (red). It has to be noted that the reduction in the transparency during contact is an effect of the force feedback gains violating (2). With local force

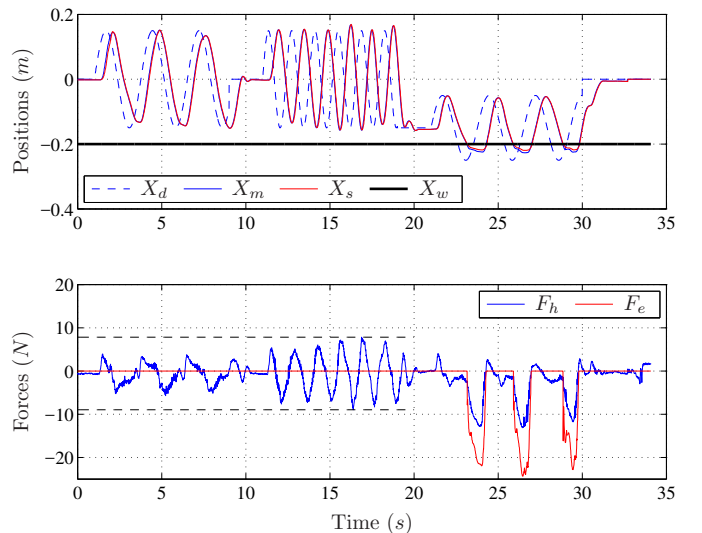


Fig. 7. Positions and forces of devices with constant local force feedback gain  $\alpha=1.4$ , with round-trip delay of 30 ms and  $C_2 = 1.0$

feedback gain, as soon as the contact stiffness is felt by the human, the force sensor measures it and feeds it back to the controller, which supports the human to push against the wall. This consequently reduces the contact stiffness felt by the human.

### 3. PROPOSED CONTROL STRATEGY

#### 3.1 Non-linear Gain Variation

Instead of having a constant gain for the local force feedback, a varying gain  $\alpha(t)$  is introduced to improve system transparency. The limitation of the constant gain approach is that the force gain reduces the contact force perceived by the operator during contacts. So, if the gain is reduced/removed when the slave makes a contact with its environment, the benefit of local force feedback during

free motion can be avoided and also this limitation during contact situations can be avoided. The proposed method is to reduce the  $\alpha$  gain with respect to the measured force of the slave-environment interaction. To do this, the measured environmental forces are sent to the master side and the gain  $\alpha(\tilde{F}_e(t))$  is varied such that is has a high value during free motion (when  $\tilde{F}_e \approx 0$ ) and has a low value when the slave interacts with the environment. Any gain variation function that results in high gain values during free slave motion and low gain values when the slave interacts with the environment can be chosen for this. Two such *purely heuristic functions* of  $\tilde{F}_e$  are illustrated in Fig. 8. The left-side plot shows a linear variation with  $\alpha^{max}$  being the maximum value achieved by the gain and  $F_e^{max}$  is chosen to be the expected upper bound for  $|\tilde{F}_e|$ , which could be the actuator force limit, for example. The right-side plot shows logistic curve where  $k$  is the steepness of the curve,  $F_{e0}$  is the  $|\tilde{F}_e|$  value of the sigmoid's midpoint and therefore,  $\alpha^{max}$  is twice the gain when  $\tilde{F}_e = F_{e0}$ . The

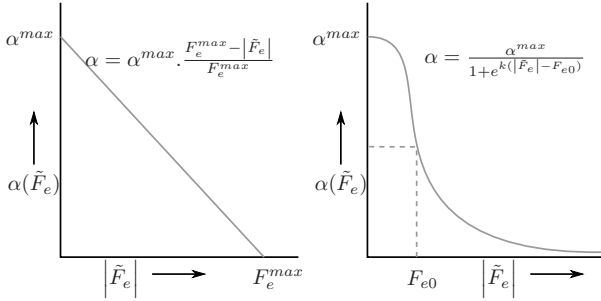


Fig. 8. Variation of the gain  $\alpha$  with the measured force signal  $\tilde{F}_e$ . The left-side plot shows a linear variation and the right-side plot shows a logistic variation.

modified network of the teleoperation system with time varying local force feedback gain is shown in Fig. 9. In this work the logistic variation of the local force feedback gain is considered and tested with hardware experiments. So, the gain varies as follows:

$$\alpha(\tilde{F}_e) = \frac{\alpha^{max}}{1 + e^{k(|\tilde{F}_e| - F_{e0})}}. \quad (3)$$

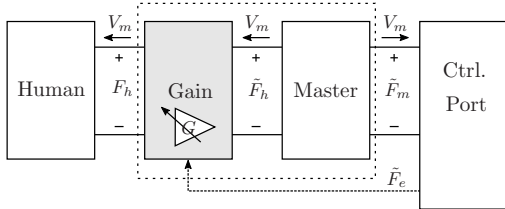


Fig. 9. The reduced model of the teleoperation system with a varying local force feedback gain. It should be noted that the  $\tilde{F}_e$  signal is shown here to represent that the gain network is modified with respect to the measured force signal received from the slave side.

#### 4. STABILITY DISCUSSION

In this section, the passivity and stability properties of the system are discussed. It is shown why the proposed

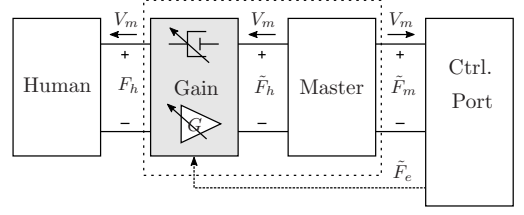


Fig. 10. The reduced model of the teleoperation system with a varying local force feedback gain and a variable damping.

method is clearly an active system and how it can be passivated which makes the overall system stable. Two methods are discussed here to ensure the passivity of the system, namely, damping injection with energy-function and with TDPA. Both the methods ensure stability of the system for any gain, independent of the variation function.

The stability problem related to time-delay has already been treated and the 4-channel bilateral controller has been stabilized using time domain passivity approach explained in Artigas et al. (2016). This means that in Fig. 9, the 1-port network of *Ctrl. Port*, which comprises of the communication channel, master and slave controller, slave device and the environment are already passivated and it results in the overall stability.

#### 4.1 System Activity

Consider the port *Gain* in Fig. 9. The power input from the human side is  $F_h V_m$  and the power output to the master device is  $\tilde{F}_h V_m$ , since only the force is amplified for the same velocity value. Clearly, this is a purely active system (unlike a power-preserving electrical transformer which amplifies voltage at its output and simultaneously reduces the current and vice-versa). The active power  $P_{active}$  can be calculated by:

$$P_{active} = \tilde{F}_h V_m - F_h V_m = \alpha F_h V_m. \quad (4)$$

The system can be made passive if at every point of time, this active power  $P_{active}$  can be dissipated. For this, a simple method is to add a virtual damping  $\gamma$  (as shown in Fig. 10) in this port which dissipates the exact amount of power, namely,  $\alpha F_h V_m$ . For the velocity  $V_m$  of the haptic device, the power dissipated by the damping  $\gamma$  is  $\gamma V_m^2$ . Therefore, the value of damping that is needed to dissipate the active power due to the force amplification is:

$$\gamma = \frac{\alpha F_h V_m}{V_m^2} = \frac{\alpha F_h}{V_m}. \quad (5)$$

This method has a limitation. The presence of  $\alpha$  in the system (although with low values when  $\tilde{F}_e$  is high) makes the port always active. To dissipate this active power, there should also always be a variable damping. This can be disturbing to the operator while he moves the haptic device. The benefit introduced by the local force feedback could be canceled out by the additional damping.

All haptic devices have some physical damping or friction (although in some devices, it is very low). Because of the friction, the haptic device considered alone is already a

dissipative system. That means, the total energy of the device keeps decreasing. In this work, this inherent passive nature of the haptic device is exploited to reduce the additional damping  $\gamma$  needed to passivate the gain port. For this, the combined port of the master and the gain is considered to analyze passivity. This combined port is shown inside the dotted rectangle in Fig. 10.

#### 4.2 Passivity by Damping Injection: Model-Based Analysis

The equation of motion of a 1-DoF haptic device with inertia  $M$ , viscous friction  $B$ , coefficient of friction  $\mu$ , local force feedback gain  $\alpha$  and additional damping  $\gamma$  is:

$$\begin{aligned} M\dot{V}_m &= \tilde{F}_h - \tilde{F}_m - (B + \gamma)V_m - \mu |F_N| \text{sgn}(V_m), \\ &= (1 + \alpha)F_h - \tilde{F}_m - (B + \gamma)V_m - \mu |F_N| \text{sgn}(V_m), \\ &= \frac{M}{\tilde{M}}F_h - \tilde{F}_m - (B + \gamma)V_m - \mu |F_N| \text{sgn}(V_m), \end{aligned} \quad (6)$$

with  $\alpha, B, \gamma, \mu \geq 0$  and  $F_N$ , the normal force.  $(1 + \alpha)$  is replaced by  $\frac{M}{\tilde{M}}$  where  $\tilde{M}$  is the apparent inertia felt by the user with the application of the force gain  $\alpha$ . So (6) can be rewritten as:

$$\tilde{M}\dot{V}_m = F_h - \frac{\tilde{M}}{M}\tilde{F}_m - \frac{\tilde{M}}{M}(B + \gamma)V_m - \frac{\tilde{M}}{M}F_\mu, \quad (7)$$

where the Coulomb friction  $F_\mu = \mu |F_N| \text{sgn}(V_m)$ . This means that when the human applies a force  $F_h$ , the apparent inertia, viscous friction, force feedback, damping and Coulomb friction felt by the user are  $\tilde{M}$ ,  $\frac{\tilde{M}}{M}B$ ,  $\frac{\tilde{M}}{M}\tilde{F}_m$ ,  $\frac{\tilde{M}}{M}\gamma$  and  $\frac{\tilde{M}}{M}F_\mu$  respectively. Let us now consider the total energy  $S$  of the master device with apparent inertia  $\tilde{M}$  and the energy change (power)  $\dot{S}$ :

$$\begin{aligned} S(V_m) &= \frac{1}{2}\tilde{M}V_m^2, \\ \dot{S}(V_m) &= V_m\tilde{M}\dot{V}_m + \frac{1}{2}\dot{\tilde{M}}V_m^2, \\ &= V_m(F_h - \frac{\tilde{M}}{M}(\tilde{F}_m + (B + \gamma)V_m + F_\mu)) + \frac{1}{2}\dot{\tilde{M}}V_m^2, \\ &= V_mF_h - \frac{\tilde{M}}{M}V_m\tilde{F}_m \\ &\quad - V_m^2(\frac{\dot{\tilde{M}}}{M}(B + \gamma) - \frac{1}{2}\dot{\tilde{M}}) - V_mF'_\mu. \end{aligned}$$

So, with  $V_mF'_\mu = \frac{\tilde{M}}{M}\mu |F_N| \text{sgn}(V_m)V_m$ , a purely dissipative term, the *perceived* 2-port of the apparent inertia with power correlated variables  $\langle F_h, V_m \rangle$  and  $\langle \frac{\tilde{M}}{M}\tilde{F}_m, V_m \rangle$  as shown in Fig. 11, is always passive, as explained by Hatanaka et al. (2015), if:

$$\frac{\dot{\tilde{M}}}{M}(B + \gamma) - \frac{1}{2}\dot{\tilde{M}} \geq 0. \quad (8)$$

Since  $\frac{M}{\tilde{M}} = (1 + \alpha)$ , the additional damping required to passivate the port can be calculated to be:

$$\gamma \geq -\frac{M\dot{\alpha}}{2(1 + \alpha)} - B. \quad (9)$$

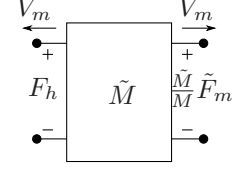


Fig. 11. 2-port of the apparent inertia

The physical interpretation of this analysis is that with time varying gain  $\alpha(\tilde{F}_e)$  for the local force feedback, the apparent inertia of the haptic device perceived by the operator becomes  $\tilde{M}$  and the feedback of the slave forces also becomes  $\frac{\tilde{M}}{M}\tilde{F}_m$  (which has a low value when  $\tilde{F}_e$  is low and a high value when  $\tilde{F}_e$  is high) which is the desired behavior of the system.

In order to find the required value of  $\gamma$  to passivate the port, the exact values of the inertia and physical damping/friction have to be identified to apply (9). Exact friction identification of a haptic device is a challenging topic by itself. This means that the additional damping  $\gamma$  required to passivate the port is subject to inaccuracies.

#### 4.3 Passivity by Damping Injection: Model-Free TDPA

The problem of friction identification can be avoided if the actual power correlated variables of the combined port of force gain block and the master device (the dotted box in Fig. 10) can be measured. By doing this, we can passivate this port by using TDPA. In classical TDPA, a passivity observer (PO) observes the energy of the system and a passivity controller (PC) is a time varying damping to dissipate energy if ever the PO observes an activity Artigas et al. (2016). Here, we modify the damping value  $\gamma$  with respect to the observed energy. Although this method is very effective, the energy accumulation problem in TDPA is widely accepted as a drawback in systems where there could be phases of passivity (which happens in the system under consideration due to the physical friction) Kim and Hannaford (2001). In order to avoid the energy accumulation issue which could make the system unstable, in this work, power based TDPA is considered for the port. This port is passive at every time step if the power leaving the port is always limited by the power entering it. The observed power (difference between input and output power) is given by:

$$P_{obs} = F_h V_m - \tilde{F}_m V_m. \quad (10)$$

This observed power has to be greater than 0 at all times. If not, it means that the power output of the system is greater than input power, which leads to activity at that time step. The power dissipated by a damping element  $\gamma$  in the system with velocity  $V_m$  is  $\gamma V_m^2$ . In order to satisfy passivity condition, we add an impedance-type PC (force modifying type), namely the damper  $\gamma$  if  $P_{obs}$  becomes negative at any point:

$$\gamma = \begin{cases} -P_{obs}/V_m^2 & \text{if } P_{obs} < 0 \\ 0 & \text{else.} \end{cases} \quad (11)$$

## 5. HARDWARE EXPERIMENTS AND RESULTS

Similar experiments described in Sec. 2.2 were conducted on the LWR-based master device equipped with a force

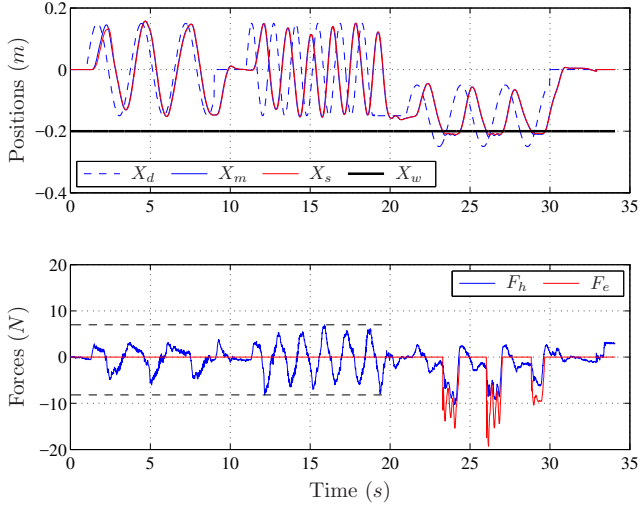


Fig. 12. With local force feedback control and without passivity checks.

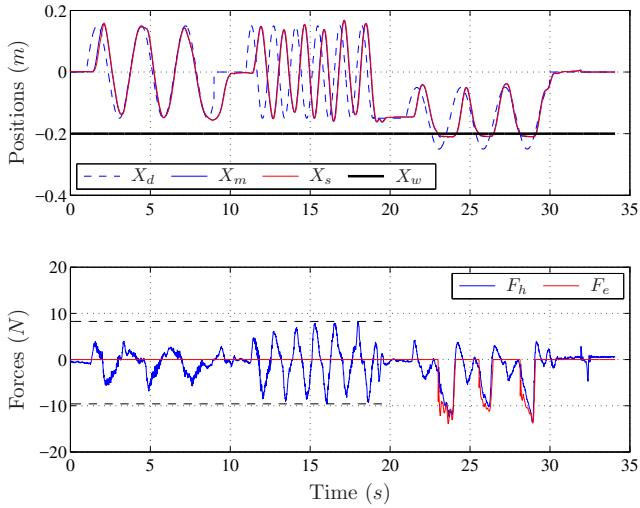


Fig. 13. With local force feedback control with model-based damping injection.

torque sensor at the end-effector. In order to produce similar experimental conditions to compare different methods, the human operator was shown a desired position trajectory (dotted blue curve in all the plots). The measured position and forces of the end-effector were used to control a virtual mass in one DoF which contacted a virtual wall, using the 4-channel bilateral controller explained in Artigas et al. (2016). For the constant local force feedback gain experiments,  $\alpha$  was tuned with fixed value of 1.4. The values of  $\alpha$  and  $\alpha^{max}$  were chosen so that the system had no disturbing high frequency force dissipation with TDPA and no oscillations with the model-based approach. For the varying gain approaches proposed in this work, the logistic variation of Fig. 8 with  $\alpha = \frac{\alpha^{max}}{1+e^{k(|\bar{F}_e|-F_{e0})}}$  with  $\alpha^{max}=1.4$ ,  $k=1$  and  $F_{e0} = 10 \text{ N}$  was selected. A round-trip delay of 30 milliseconds was simulated between the master and slave devices. Fig. 12 shows the positions and forces of the devices with varying gain approach without any passivity checks which gets unstable during wall contacts. Note that the virtual wall is placed at a distance of 20 centimeters. The desired trajectory has 3 parts: a low frequency ( 0.36

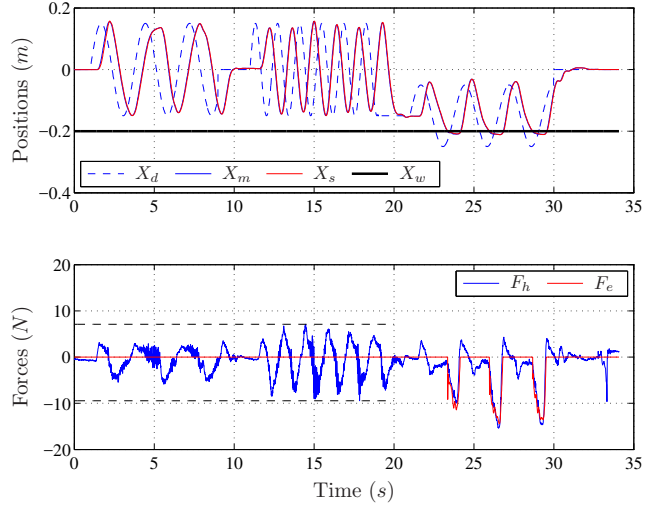


Fig. 14. With local force feedback control passivated using TDPA.

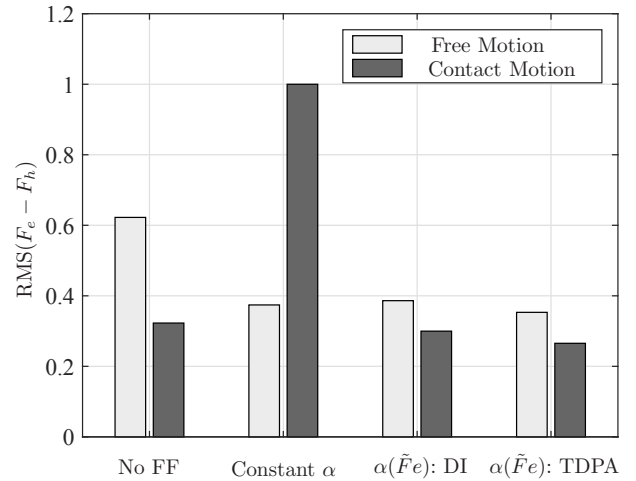


Fig. 15. Bar plots of normalized root mean square errors of the forces  $F_e$  and  $F_h$  values for values for all the methods.

Hz) free slave motion, a higher frequency (0.72 Hz) free slave motion and a low frequency motion where the slave hits the virtual wall. The same test was done with passivity checks and damping injection using the energy function and TDPA.

The resulting positions and forces are shown in Fig. 13 and Fig. 14 respectively. It can be seen that when the system is rendered passive with any of the proposed methods, during free motion, the forces felt by the human are lower than the case when there was no local feedback (compare this with Fig. 6). During wall contacts, the human feels almost the same force as measured by the slave device, which corresponds to an improved performance when compared to the constant gain approach shown in Fig. 7.

Still the proposed methods have certain limitations. The model based damping injection method is highly dependent on the identification of the system parameters. TDPA based approach introduces high frequency force modification (it is slightly seen in Fig. 14) which can be disturbing to the operator. This effect can be removed by using low-order passive force filters.

In order to evaluate the performance improvement of the proposed methods, the root mean square error (RMSE) between the measured environment force  $F_e$  and the force felt by the human,  $F_h$  is calculated for all the cases and displayed in Fig. 15 in a normalized form. As it can be seen, without local force feedback, the error between  $F_h$  and  $F_e = 0$  during free motion is higher since the human feels the inertia and damping of the master device. But during contact, the error value is low since there is no local feedback and therefore, the human perceives the slave environment with higher stiffness. As expected, with the introduction of a constant gain for the local force feedback, the perceived inertia and damping of the haptic device are highly reduced and the RMSE value is lower. Since the constant gain reduces the environment stiffness felt by the human, the RMSE during contact motion is higher. The proposed methods (with damping injection and TDPA) improve the performance of the system in both free motion and during contacts as shown by low RMSE values. These plots validate the effectiveness of the proposed methods and clearly show that the benefits of both the earlier approaches (high stiffness during contacts from "No FF" and low inertia and damping during free motion from "Constant  $\alpha$ ") can be availed for a better teleoperation performance.

## 6. CONCLUSION AND FUTURE WORK

For a teleoperation system without communication delay, it was shown that high levels of transparency can be achieved with local force feedback. Although it helps reduce the apparent inertia and damping in free slave motion, it also reduces the contact stiffness perceived by the user significantly for systems with delays, because environmental force feedback gains are limited due to stability issues. A new time varying gain (but one that avoids instantaneous switching) for the local force feedback was proposed as a function of the measured environmental forces. Stability of the system is ensured using damping injections with two approaches, namely, model-based energy function and time domain passivity approach. Hardware experiments on a KUKA light-weight-robot-based haptic interface showed significant increase in performance of the system while using the new approaches. This paper presents only the initial results of the proposed methods. Selection of better local force feedback gain functions and stability methods, optimized extension of the proposed methods to all the DoFs of the haptic interface and a deeper statistical analysis with a user-study to evaluate and understand the system behavior are works envisaged by the authors.

## REFERENCES

- Abdossalami, A. and Sirouspour, S. (2008). Adaptive control of haptic interaction with impedance and admittance type virtual environments. In *Haptic interfaces for virtual environment and teleoperator systems, 2008. haptics 2008. symposium on*, 145–152. IEEE.
- Artigas, J., Balachandran, R., Riecke, C., Stelzer, M., Weber, B., Ryu, J.H., and Albu-Schaeffer, A. (2016). Kontur-2: force-feedback teleoperation from the international space station. In *2016 IEEE International Conference on Robotics and Automation (ICRA)*. IEEE.
- Colgate, J.E. (1993). Robust impedance shaping telemanipulation. *IEEE Transactions on robotics and automation*, 9(4).
- Gil, J.J., Rubio, A., and Savall, J. (2009). Decreasing the apparent inertia of an impedance haptic device by using force feedforward. *IEEE Transactions on Control Systems Technology*.
- Hashtrudi-Zaad, K. and Salcudean, S.E. (2002). Transparency in time-delayed systems and the effect of local force feedback for transparent teleoperation. *IEEE Transactions on Robotics and Automation*, 18(1), 108–114.
- Hashtrudi-Zaad, K. and Salcudean, S. (1999). On the use of local force feedback for transparent teleoperation. In *Robotics and Automation, 1999. Proceedings. 1999 IEEE International Conference on*, volume 3, 1863–1869. IEEE.
- Hatanaka, T., Chopra, N., Fujita, M., and Spong, M.W. (2015). Foundation: Passivity, stability and passivity-based motion control. In *Passivity-Based Control and Estimation in Networked Robotics*. Springer.
- Hokayem, P.F. and Spong, M.W. (2006). Bilateral teleoperation: An historical survey. *Automatica*, 42(12), 2035–2057.
- Hulin, T., Hertkorn, K., Kremer, P., Schätzle, S., Artigas, J., Sagardia, M., Zacharias, F., and Preusche, C. (2011). The dlr bimanual haptic device with optimized workspace. In *Robotics and Automation (ICRA), 2011 IEEE International Conference on*, 3441–3442. IEEE.
- Ishii, T. and Katsura, S. (2012). Bilateral control with local force feedback for delay-free teleoperation. In *Advanced Motion Control (AMC), 2012 12th IEEE International Workshop on*, 1–6. IEEE.
- Kaneko, K., Tokashiki, H., Tanie, K., and Komoriza, K. (1998). Macro-micro bilateral teleoperation based on operational force feedforward. *IEEE Transactions on Robotics and Automation*, 1761–1769.
- Kim, Y.S. and Hannaford, B. (2001). Some practical issues in time domain passivity control of haptic interfaces. In *Intelligent Robots and Systems, 2001. Proceedings. 2001 IEEE/RSJ International Conference on*, volume 3, 1744–1750. IEEE.
- Niemeyer, G. and Slotine, J.J. (1991). Stable adaptive teleoperation. *Oceanic Engineering, IEEE Journal of*, 16(1), 152–162.
- Panzirsch, M., Hulin, T., Artigas, J., Ott, C., and Ferre, M. (2016). Integrating measured force feedback in passive multilateral teleoperation. In *International Conference on Human Haptic Sensing and Touch Enabled Computer Applications*, 316–326. Springer.
- Tobergte, A., Helmer, P., Hagn, U., Rouiller, P., Thielmann, S., Grange, S., Albu-Schäffer, A., Conti, F., and Hirzinger, G. (2011). The sigma. 7 haptic interface for mirosurge: A new bi-manual surgical console. In *Intelligent Robots and Systems (IROS), 2011 IEEE/RSJ International Conference on*, 3023–3030. IEEE.
- Ueberle, M. and Buss, M. (2002). Design, control, and evaluation of a new 6 dof haptic device. *IEEE Transactions on Robotics and Automation*.